

TERAHERTZ RADIATION

https://doi.org/10.1070/QEL16806

Mode loss spectra in THz quantum-cascade lasers with gold- and silver-based double metal waveguides

D.V. Ushakov, A.A. Afonenko, A.A. Dubinov, V.I. Gavrilenko, I.S. Vasil'evskii, N.V. Shchavruk, D.S. Ponomarev, R.A. Khabibullin

Abstract. **Spectra of the waveguide loss coefficient for THz radiation of a quantum-cascade laser with a gold- and silver-based double metal waveguide (DMW) are calculated based on the measurements of resistivity of the metals for different temperatures. It is shown that, taking into account the absorption of THz radiation by free carriers and optical phonons, the spectrum of total mode losses has a broad minimum in the range of 3–6 THz, which shifts to higher frequencies with increasing temperature. The minimum losses in the Au-based waveguide increase from 8 to 27 cm^{-1} as temperature increases from 100 to 300 K. The use of an Ag-based DMW makes it possible to decrease the losses by 2–4 cm^{-1} compared to the Au-based DMW.**

Keywords: *double metal waveguide, loss coefficient, quantum-cascade lasers, terahertz region.*

1. Introduction

Most efficient operation in the THz region is demonstrated by quantum-cascade lasers (QCLs) with a double metal waveguide (DMW) having an active region sandwiched between two metal layers [1]. The optical confinement factor in these waveguides is $\Gamma \sim 1$, which is considerably higher than in plasmon waveguides ($\Gamma \sim 0.3$), which efficiently operate in mid-IR QCLs. However, QCLs with DMWs are difficult to fabricate [2] and require preliminary theoretical and experimental investigations of the behaviour of the dielectric constant and loss coefficient of both metals and semiconductors in the THz spectral region [3].

D.V. Ushakov, A.A. Afonenko Belarusian State University, prosp. Nezavisimosti 4, 220030 Minsk, Belarus; e-mail: UshakovDV@bsu.by;
A.A. Dubinov Institute for Physics of Microstructures, Federal Research Center 'Institute of Applied Physics", Russian Academy of Sciences, Akademicheskaya ul. 7, d. Afonino, 603087 Kstovskii raion, Nizhny Novgorod region, Russia; N.I. Lobachevsky State University of Nizhny Novgorod (National Research University), prosp. Gagarina 23, 603950 Nizhny Novgorod, Russia;
V.I. Gavrilenko Institute for Physics of Microstructures, Federal Research Center 'Institute of Applied Physics', Russian Academy of Sciences, Akademicheskaya ul. 7, d. Afonino, 603087 Kstovskii raion, Nizhny Novgorod region, Russia;
I.S. Vasil'evskii National Research Nuclear University 'MEPhI', Kashirskoe sh. 31, 115409 Moscow, Russia;
N.V. Shchavruk, D.S. Ponomarev, R.A. Khabibullin V.G. Mokerov Institute of Ultrahigh Frequency Semiconductor Electronics, Nagornyi proezd 7, stroenie 5, 117105 Moscow, Russia

Received 30 August 2018
Kvantovaya Elektronika **48** (11) 1005–1008 (2018)
Translated by M.N. Basieva

To develop more efficient working schemes of QCLs and a more elaborate design of THz waveguides, one needs information about losses in THz QCLs in wide temperature and frequency ranges [4]. For example, the use of Cu claddings for a DMW allowed one to decrease the losses and increase the maximum working temperature of pulsed THz QCLs approximately to 200 K [5]. In addition, it was shown that losses in these QCLs play an important role in the intrinsic frequency tuning [6].

The aim of the present work is to study the spectra of mode losses in THz QCLs with gold- and silver-based DMWs. Of special interest are THz lasers with a DMW based on silver, because this metal has higher electric and thermal conductivities than gold and copper, which should lead to lower losses in Ag-based waveguides. In addition, the use of Ag as one of the waveguide claddings was successfully demonstrated for IR [7] and THz [3] QCLs.

2. Dielectric constant of DMW claddings

The dielectric constant of metals in the THz spectral region is usually described according to the Drude model as

$$\varepsilon = 1 - \frac{\omega_p^2}{\omega(\omega + i\gamma_d)}, \tag{1}$$

where

$$\omega_p = \left(\frac{ne^2}{m\varepsilon_0}\right)^{1/2} \tag{2}$$

is the plasma frequency, n is the free-electron concentration, e is the electron charge, m is the effective electron mass, ε_0 is the vacuum dielectric constant, and γ_d is the damping parameter. The values of $\hbar\omega_p$ were calculated to be 9.02 eV for Au and 8.98 eV for Ag, which well agree with the data of [8]. The available data on the parameter γ_d widely vary in the literature [8–11] and depend on the considered frequency range and the metal film deposition temperature. This parameter is directly proportional to resistivity ρ, i.e.,

$$\gamma_d = ne\rho/m. \tag{3}$$

Thus, to determine γ_d, it is necessary to experimentally measure the resistivity of metal claddings as a function of temperature [9, 10]. For this purpose, we resistively deposited Ti/Au (30/1000 nm) and Ti/Ag (30/1000 nm) layers on a semi-insulating GaAs substrate in a vacuum chamber with technological regimes used for fabricating THz QCLs [2, 12].

The obtained samples were cleaved along crystallographic axes into square pieces with dimensions ~1 × 1 cm, and then their resistivity ($\rho = 1/\sigma$) was measured by the Van der Pauw method within the temperature range from 4.2 to 300 K.

Figure 1 presents the experimental dependence of resistivity ρ on temperature T for Au and Ag films. The resistivity of Ag at $T = 300$ K (2.18 μΩ cm) is 1.5-fold lower than the resistivity of Au (3.25 μΩ cm). The measured ρ for the Au and Ag films are higher than the values obtained for bulk samples of these metals, which is related to a larger contribution from surface scattering [13].

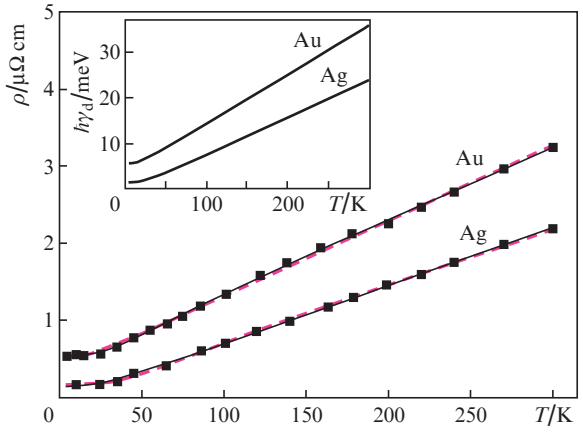

Figure 1. Temperature dependences of resistivity ρ for Au and Ag films [points present experimental data, solid curves belong to calculation by Grüneisen formula (4), and dashed curves correspond to calculations based on simplified formula (5)]. The inset shows the temperature dependences of damping energy $\hbar\gamma_d$ for Au and Ag films.

The obtained temperature dependences of resistivity allow one to determine the Debye temperature T_D using the Grüneisen formula [9]

$$\rho(T) = \rho_0 + \frac{\rho_1}{\tilde{T}^5}\int_0^{\tilde{T}} \frac{x^5 dx}{(e^x - 1)(1 - e^{-x})}, \quad (4)$$

where ρ_0 and ρ_1 are the residual and characteristic resistivity and $\tilde{T} = T_D/T$ is the reduced temperature. One can see from Fig. 1 that the experimental data well coincide with the theoretical curves at $T_D = 160.0$ K for Au and 220.6 K for Ag. The found T_D well agree with the literature data for bulk metals, which are 178 and 221 K for Au and Ag, respectively [14].

Taking into account the dominant role of the phonon scattering mechanism, the temperature dependence of the resistivity can be described by the simplified formula

$$\rho(T) = \rho_0 + \frac{\rho_1}{e^{T_{ch}/T} - 1}, \quad (5)$$

where T_{ch} is the characteristic temperature. Calculation by formula (5) also yields good agreement with the experimental data (see Fig. 1). Taking into account the linear relation between the resistivity and the damping energy, we find from formula (3)

$$\gamma_d(T) = \frac{ne^2}{m}\rho(T) = \gamma_{d0} + \frac{\gamma_{d1}}{e^{T_{ch}/T} - 1}, \quad (6)$$

where γ_{d0} and γ_{d1} are the residual and characteristic damping parameters, respectively.

The approximation parameters in formulas (5) and (6) were found based on root-mean-square error minimisation and are presented in Table 1. Calculations by formula (6) (see the inset in Fig. 1) show that damping energy $\hbar\gamma_d$ for Au is 14.3 meV at $T = 100$ K and 25 meV at $T = 200$ K and almost linearly increases with increasing temperature with a factor $\hbar\gamma_{d1}/T_{ch} = 0.107$ meV K^{-1}. The damping energy for Ag is $\hbar\gamma_d = 7.5$ meV at $T = 100$ K and 15.7 meV at $T = 200$ K and increases with temperature with $\hbar\gamma_{d1}/T_{ch} = 0.080$ meV K^{-1}.

3. DMW cladding loss coefficient

The results of calculations of the loss coefficient at the Au and Ag layers (α_{met}) based on formulae (1), (5), and (6) are presented in Fig. 2. One can see that the loss coefficient increases with increasing frequency and temperature. In particular, at a frequency of 3 THz and temperatures of 50, 100, 150, 200, 250, and 300 K, the coefficient α_{met} for Au DMW layers is equal to 3.3, 4.9, 6.3, 7.6, 8.7, and 9.8 cm^{-1}, respectively, while this coefficient for Ag layers at the same frequencies and temperatures is 1.4, 2.7, 4.1, 5.3, 6.4, and 7.4 cm^{-1}. Figure 2 shows that the losses at Ag layers at 250 K are close to the losses at Au layers at 150 K for the entire considered frequency region. Thus, the use of silver for DMW wafers allows one to decrease the α_{met} by more than 2 cm^{-1} and increase the maximum ope-

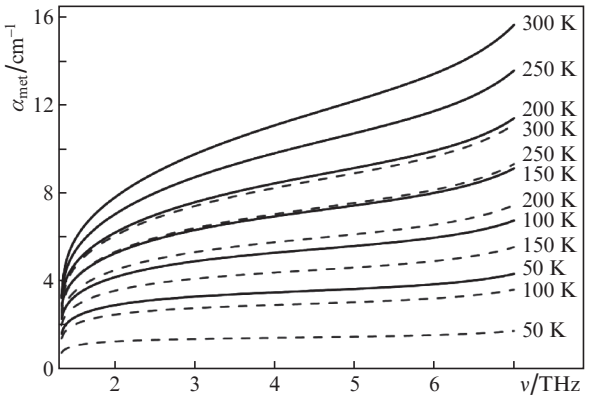

Figure 2. Dependences of loss coefficient at claddings of Au- (solid curves) and Ag-based (dashed curves) DMWs on frequency ν at temperatures from 50 to 300 K.

Table 1. Parameters used to calculate the dielectric constant and resistivity of Au and Ag films.

Metal	n/cm^{-3}	$\hbar\omega_p$/eV	ρ_0/μΩ cm	ρ_1/μΩ cm	$\hbar\gamma_{d0}$/meV	$\hbar\gamma_{d1}$/meV	T_{ch}/K
Au	5.9×10^{22}	9.02	0.51	0.40	5.6	4.3	40.2
Ag	5.85×10^{22}	8.98	0.14	0.48	1.5	5.2	62.3

rating temperature of THz QCLs compared to the laser based on a DMW with gold claddings.

4. Total loss coefficient in a THz QCLs with a DMW

The total loss coefficient, which includes losses at the DMW claddings, at cavity mirrors, and due to absorption by optical phonons and free charge carriers, was calculated for a waveguide 10 μm thick. In calculations, we considered the QCL active region containing 228 cascades based on the resonance-phonon design [15, 16]. One cascade consists of a sequence of three GaAs quantum wells separated by $Al_{0.15}Ga_{0.85}As$ barrier layers [17, 18]. The QCL active region is sandwiched between two n^+ GaAs contact layers 50 nm thick with a dopant concentration of 5×10^{18} cm^{-3}.

The waveguide characteristics were calculated for the TM mode with the use of the numerical solution of the waveguide equation for the nonzero magnetic field component H_y taking into account the relation with the E_x and E_z electric field components:

$$\varepsilon(x)\frac{\partial}{\partial x}\frac{1}{\varepsilon(x)}\frac{\partial H_y}{\partial x}+\left[\varepsilon(x)\frac{\omega^2}{c^2}-\beta^2\right]H_y=0,$$
$$E_x=\frac{\beta}{\varepsilon_0\varepsilon(x)\omega}H_y,\quad E_z=\frac{\mathrm{i}}{\varepsilon_0\varepsilon(x)\omega}\frac{\partial H_y}{\partial x}. \tag{7}$$

At the interfaces of layers, the conditions of continuity of tangential components E_x and E_z are fulfilled.

The expression for the semiconductor dielectric constant, which contains the phonon component and a term corresponding to the absorption of light by free carriers, can be presented in the form [19]

$$\varepsilon=\varepsilon_\mathrm{b}+\frac{(\varepsilon_\mathrm{low}-\varepsilon_\infty)\omega_\mathrm{TO}^2}{\omega(\omega+\mathrm{i}\gamma_\mathrm{d}^\mathrm{TO})-\omega_\mathrm{TO}^2}-\frac{\omega_\mathrm{p}^2}{\omega(\omega+\mathrm{i}\gamma_\mathrm{d}^\mathrm{GaAs})}. \tag{8}$$

For numerical calculations, the values of the background (ε_b), low-frequency (ε_low), and high-frequency (ε_∞) dielectric constant components, optical phonon damping parameters ($\gamma_\mathrm{d}^\mathrm{TO}$), and absorption by free carriers ($\gamma_\mathrm{d}^\mathrm{GaAs}$) are taken from [19, 20]. The temperature dependence of the damping energy of semiconductor layers was calculated by the formula

$$\gamma_\mathrm{d}^\mathrm{GaAs}(T)=\frac{e}{m_\mathrm{c}\mu(T)}, \tag{9}$$

where m_c is the effective electron mass in the conduction band of semiconductor layers and $\mu(T)$ is the temperature-dependent electron mobility. The dependence of the mobility on temperature and impurity concentration for GaAs/$Al_xGa_{1-x}As$ layers was determined based on the experimental data using interpolation formulas from [21].

In addition to waveguide mode losses, we took into account the losses due to reflection from mirrors. Due to the long QCL wavelength (~100 μm) compared to the waveguide thickness (~10 μm), coupling out of radiation is hindered, and the reflection coefficient is close to unity. The losses for a cavity 1 mm long and reflection coefficient $R = 0.9$ were 1 cm^{-1}.

Numerical calculations (Fig. 3) show that the loss coefficient α nonmonotonically changes with frequency. In the low-frequency range ($\nu < 3$ THz), the losses increase due to absorption of light by free carriers, while the increase in losses in the region with $\nu > 6$ THz is caused by the resonance absorption by TO phonons $\hbar\omega_\mathrm{TO} = 33.5$ meV. As is seen from Fig. 3 that the loss coefficient α increases with increasing temperature. In addition, an increase in temperature leads to a sharp increase of α in the high- and low-frequency regions. The spectrum of total losses has a broad minimum in the range of 3–6 THz.

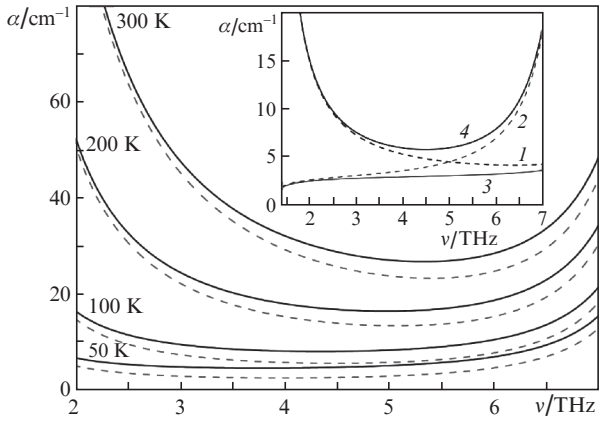

Figure 3. THz spectra of the loss coefficient in QCLs with DMWs based on Au (solid curves) and Ag (dashed curves) at different temperatures. The inset shows the loss coefficient components for a QCL with an Ag-based DMW at $T = 100$ K related to the absorption of light by free carriers (*1*), by optical phonons (*2*) and in metal claddings (*3*), as well as the total loss coefficient (*4*).

Table 2 lists minimum α and corresponding frequencies for THz QCLs with Au- and Ag-based DMWs for different temperatures. An increase in temperature from 50 to 300 K leads to an increase in minimum losses from 4.8 to 27.0 cm^{-1} for Au layers and from 2.7 to 23.4 cm^{-1} for Ag layers. At the same time, the contribution of the DMW absorption changes from 73% to 48% in the case of Au layers and from 52% to 39% for Ag layers. The presented data indicate that the use of Ag-based DMWs allows one to decrease losses by 2.1, 2.4, 3.0, and 3.6 cm^{-1} at $T = 50$, 100, 200, and 300 K, respectively, in comparison with the Au-based DMW.

Table 2. Positions of minimum α in the THz spectrum of QCLs with Au- and Ag-based DMWs at different temperatures.

Au			Ag		
T/K	ν/THz	α/cm^{-1}	T/K	ν/THz	α/cm^{-1}
50	3.8	4.8	50	4.0	2.7
100	4.3	8.2	100	4.5	5.8
200	5.0	16.6	200	5.1	13.6
300	5.3	27.0	300	5.4	23.4

It should be noted that, as temperature increases from 50 to 300 K, the minimum α shifts to higher frequencies, namely, from 3.8 to 5.3 THz for Au-based DMWs and from 4.0 to 5.4 THz for Ag-based DMWs. Thus, the use of silver for DMW claddings makes it possible to increase the efficiency and improve the temperature characteristics of THz QCLs emitting at frequencies exceeding 4 THz.

Acknowledgements. This work was supported by the Russian Foundation for Basic Research (Grant Nos 17-02-00070 A and 18-52-00011_Bel) and by the Belarusian Republican Foundation for Basic Research (Grant No. F18P-107). The experimental part of the work (fabrication of samples and measurement of resistivity of metal films) performed by N.V. Shchavruk, D.S. Ponomarev, and A.A. Dubinov was supported by the Russian Science Foundation (Grant No. 18-19-00493).

References

1. Unterrainer K., Colombelli R., Gmachl C., Capasso F., Hwang H.Y., Sergent A.M., Sivco D.L., Cho A.Y. *Appl. Phys. Lett*., **80**, 3060 (2002).
2. Khabibullin R.A., Shchavruk N.V., Pavlov A.Yu., Ponomarev D.S., Tomosh K.N., Galiev R.R., Mal'tsev P.P., Zhukov A.E., Tsyrlin G.E., Zubov F.I., Alferov Zh.I. *Fiz. Tekh. Poluprovodn*., **50**, 1395 (2016).
3. Han Y.J., Li L.H., Zhu J., Valavanis A., Freeman J.R., Chen L., Rosamond M., Dean P., Davies A.G., Linfield E.H. *Opt. Express*, **26**, 3814 (2018).
4. Martl M., Darmo J., Deutsch C., Brandstetter M., Andrews A.M., Klang P., Strasser G., Unterrainer K. *Opt. Express*, **19**, 733 (2011).
5. Fathololoumi S., Dupont E., Chan C.W.I., Wasilewski Z.R., Laframboise S.R., Ban D., Matyas A., Jirauschek C., Hu Q., Liu H.C. *Opt. Express*, **20**, 3866 (2012).
6. Schrottke L., Lu X., Roben B., Biermann K., Wienold M., Richter H., Hubers H.W., Grahn H.T. *J. Appl. Phys*., **123**, 213102 (2018).
7. Bahriz M., Moreau V., Palomo J., Colombelli R., Austin D.A., Cockburn J.W., Wilson L.R., Krysa A.B., Roberts J.S. *Appl. Phys. Lett*., **88**, 181103 (2006).
8. Ordal M.A., Long L.L., Bell R.J., Bell S.E., Bell R.R., Alexander R.W., Ward C.A. *Appl. Opt*., **22**, 1099 (1983).
9. Johnson P.B., Christy R.W. *Phys. Rev. B*, **6**, 4370 (1972).
10. Ordal M.A., Bell R.J., Alexander R.W., Long L.L., Querry M.R. *Appl. Opt*., **24**, 4493 (1985).
11. Babar S., Weaver J.H. *Appl. Opt*., **54**, 477 (2015).
12. Ikonnikov A.V., Marem'yanin K.V., Morozov S.V., Gavrilenko V.I., Pavlov A.Yu., Shchavruk N.V., Khabibullin R.A., Reznik R.R., Tsyrlin G.E., Zubov F.I., Zhukov A.E., Alferov Zh.I. *Pis'ma Zh. Tekh. Fiz*., **43**, 86 (2017).
13. Cheng Z., Liu L., Xu S., Lu M., Wang X. *Sci. Rep*., **5**, 10718 (2015).
14. Ho C.Y., Powell R.W., Liley P.E. *J. Phys. Chem. Ref. Data*, **3**, 1 (1974).
15. Khabibullin R.A., Shchavruk N.V., Ponomarev D.S., Ushakov D.V., Afonenko A.A., Vasil'evskii I.S., Zaitsev A.A., Danilov A.I., Volkov O.Yu., Pavlovskii V.V., et al. *Fiz. Tekh. Poluprovodn*., **52**, 1268 (2018).
16. Volkov O.Yu., Dyuzhikov I.N., Logunov M.V., Nikitov S.A., Pavlovskii V.V., Shchavruk N.V., Pavvov A.Yu., Khabibullin R.A. *Radiotekh. Elektron*., **63**, 981 (2018).
17. Khabibullin R.A., Shchavruk N.V., Klochkov A.N., Glinskii I.A., Zenchenko N.V., Ponomarev D.S., Mal'tsev P.P., Zaitsev A.A., Zhukov A.E., Tsyrlin G.E., Alferov Zh.I. *Fiz. Tekh. Poluprovodn*., **51**, 540 (2017).
18. Reznik R.R., Kryzhanovskaya N.V., Zubov F.I., Zhukov A.E., Khabibullin R.A., Morozov S.V., Cirlin G.E. *J. Phys.: Conf. Series*, **917**, 052012 (2017).
19. Moore W.J., Holm R.T. *J. Appl. Phys*., **80**, 6939 (1996).
20. Blakemore J.S. *J. Appl. Phys*., **53**, R123 (1982).
21. Chin V.W.L., Osotchan T., Vaughan M.R., Tansley T.L., Griffiths G.J., Kachwalla Z. *J. Electron. Mater*., **22**, 1317 (1993).